

Rapporto attività LNF 2015

NA62

**A. Antonelli (Resp.), F. Gonnella (AR), G. Lamanna,
V.Kozhuharov (associato), G.Mannocchi (associato), M.Moulson, M.Raggi
(Art.36,), T.Spadaro
In collaboration with
E. Capitolo, R. Lenci, V. Russo,
S.Valeri, T. Vassilieva
the Servizio di Progettazione Apparati Sperimentali (SPAS)
C. Capoccia, A. Cecchetti
the Servizio di Sviluppo e Costruzione Rivelatori (SSCR)
G. Bisogni, A. Franceschi
the Divisione Acceleratori, Servizio di Vuoto
V. Lollo
and the Servizio di Elettronica
G. Corradi, D. Tagnani.**

The NA62 Experiment

The branching ratio (BR) for the decay $K^+ \rightarrow \pi^+ \nu \bar{\nu}$ can be related to the value of the CKM matrix element V_{td} with minimal theoretical uncertainty, providing a sensitive probe of the flavor sector of the Standard Model. The goal of the NA62 experiment at the CERN SPS is to detect ~ 100 decays $K^+ \rightarrow \pi^+ \nu \bar{\nu}$ with a S/B ratio of 10:1.

The experiment makes use of a 75 GeV unseparated positive secondary beam. The total beam rate is 800 MHz, providing ~ 50 MHz of K^+ 's. The decay volume begins 102 m downstream of the production target. 5 MHz of kaon decays are observed in the 65-m long fiducial vacuum decay region. Ring-shaped large-angle photon vetoes (LAVs) are placed at 12 stations along the decay region and provide full coverage for decay photons with $8.5 \text{ mrad} < \theta < 50 \text{ mrad}$. The last 35m of the decay region hosts a dipole spectrometer with four straw-tracker stations operated in vacuum. The NA48 liquid-krypton calorimeter (LKr) is used to veto high-energy photons at small angle. Additional detectors further downstream extend the coverage of the photon veto system (e.g. for particles traveling in the beam pipe).

LNF group activity: Large Angle Veto detectors

The principal achievements of the photon-veto working group in 2015 were in the commissioning of the Large-Angle Veto (LAV) system, which is a responsibility of the LNF group responsibility, as well as providing general support to the experiment, assisting with run planning and coordination, and participating in data taking.

Particular progress on the LAV system was made in the following areas:

- Development of the level-zero trigger firmware.
- Implementation and optimization of the reconstruction code.
- Analysis of 2014 data and measurement of system performance.

The LAV system consists of 12 detector stations arranged at intervals of 6 to 10 m along the vacuum tank along its entire length. The first 11 stations are incorporated into the tank itself and are operated in vacuum; the 12th station is placed immediately downstream of the RICH and is operated in air. The diameter of the stations increases with distance from the target, as does the number of blocks in each, from 160 to 256, for a total of 2496 blocks. Each station consists of four or five rings of blocks, with the blocks staggered in azimuth in successive rings. The total depth of a five-layer station is 27 radiation lengths. This structure guarantees high efficiency, hermeticity, and uniformity of response.

The first LAV station, A1, was constructed in 2009 and served as a prototype. By August 2014, all twelve stations were completed, delivered to CERN and installed on the beam line. During the construction of the LAV detectors, more than 2500 lead-glass blocks from the OPAL electromagnetic barrel calorimeter were processed (structurally reinforced, cleaned, fitted with new HV dividers, tested, and characterized).

The particles traversing the LAV detectors mainly consist of photons from kaon decays, as well as muons and pions in the beam halo. For each incoming particle, the veto detectors are expected to provide a time measurement with 1-ns resolution and an energy measurement of moderate precision (of order 10%). To maintain the detection efficiency as high as possible for muons and low energy photons, the system must be operated with thresholds of a few millivolts, i.e., well below the signal amplitude for minimum-ionizing particles (MIP). With an intrinsic time resolution of < 1 ns for the lead-glass blocks and a rise time of 5 ns for the Hamamatsu R2238 PMTs, the requirements on the precision of the time measurement are not difficult to satisfy. On the other hand, the amount of energy deposited in the LAV stations for photons from π^0 decays spans a very wide range, from about 100 MeV up to 30 GeV. Using the measured average photoelectron yield of 0.3 p.e./MeV and a nominal gain of 1×10^6 for the R2238 PMT, one expects a signal charge of 4.5 pC for a MIP, corresponding to a signal amplitude of 20 mV on a 50 load. At the upper end of the photon energy range, signals from 20 GeV showers can reach an amplitude of 10V. The readout chain for the LAV stations consists of two different types of boards, a dedicated front-end board (LAV-FEE) developed for the LAV detector, and a common digital readout board called TEL62, used by many of the NA62 detectors.

The LAV-FEE board, a custom 9U board designed by the LNF Servizio di

Elektronika, splits the analog signal from the PMT into two copies and converts each into a logical LVDS signal, using two comparators with independently adjustable thresholds. The duration of the LVDS pulse is equal to the time during which the analog signal is above the programmed threshold. The basic idea is to exploit the time-over-threshold (ToT) technique to measure the signal charge over a broad interval. The LVDS signals are then sent to the TEL62 readout board, in which a custom-designed TDC mezzanine digitizes each signal into leading and trailing times. The FPGAs on board the TEL62 are used to correct raw hit times for slewing and to produce a level-zero (L0) trigger primitive, which is sent to the L0 trigger processor using a dedicated Gigabit Ethernet interface. The system is designed to sustain hit rates of up to 100 kHz per channel and to be able to transmit a data volume to the L1 PC farm of up to 2.4 Gbit/s for each station.

During the 2014-2015 runs, there was significant progress on the implementation of the L0 trigger for the LAV system. The NA62 L0 trigger receives inputs, or “primitives”, from each detector system. These are generated by the FPGAs on the TEL62 boards, which examine buffered data during acquisition, and then forwarded to the central L0 trigger processor, which decides whether to initiate readout. The LAV12 L0 firmware reconstructs physical hits by searching for matching leading edges on the low- and high-threshold channels of each block within a programmable coincidence window, nominally 6 ns; if a coincidence is found, a slewing correction is applied to obtain the hit time. The hits are sorted and hits within a programmable window up to 25 ns in length are merged. The primitive, if generated, contains the timestamp of the acquisition window to read out; the time resolution is 100 ps.

Primitives are continuously generated with a rate of up to 10 MHz, and during the 2015 run were used as a zero-bias monitor of the activity on LAV12. As illustrated in Fig. LAV-1, the spill structure is evident in the LAV12 primitive rate. During the 2014 run, the L0 primitives provided the first evidence for the 75-Hz microstructure in the spill seen in the zoom in the bottom panel of the figure.

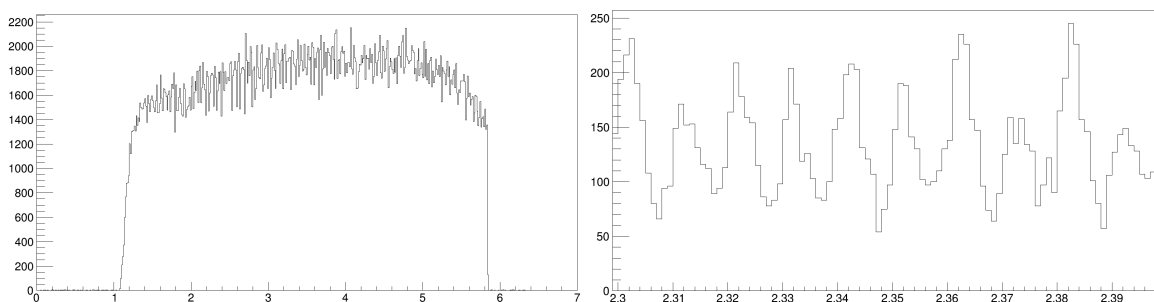


Figure LAV-1. Continuous monitoring of LAV12 hits from L0 trigger primitives, in bins of 0.5 s (left), and zoom in bins of 0.02 s (right), showing evidence of 75-Hz spill structure.

Much progress has been made on the LAV reconstruction code and on the data analysis. The performance of the LAV system has been studied both with data

collected under standard conditions, i.e., with a trigger based on the identification of K^+ decay products, and during dedicated muon runs, with the beam dump closed and the muon-sweeping magnets turned off, so that the experiment is traversed only by high-energy muons that penetrate the upstream shielding.

Muon runs were used to establish the threshold settings and to study the efficiency for the reconstruction of hits left by MIPs. Penetrating muon “tracks” in the LAV system were identified by the correlation between hits on blocks at the same azimuthal angle in different stations, as illustrated in Fig. LAV-2; for certain configurations, it is additionally possible to require hits on the blocks immediately upstream and downstream of a given block in order to better determine its efficiency. We find that the MIP detection efficiency saturates for values of the low threshold below 6 mV. This led us to adopt a value of 5 mV for the low-threshold working point, as seen in Fig. LAV-3.

Runs in standard conditions are used to measure the time offsets for each channel with respect to the signals from the detectors that provide the experiment’s event-time reference (CHOD and KTAG). Hit reconstruction is then performed and slewing corrections are applied. A hit may be reconstructed from up to four time measurements, corresponding to the leading- and trailing-edge times on each of the high and low thresholds. The algorithm used to correct for slewing depends on how many and which of the edges are used to reconstruct the hit. For example, if both leading edges are present, the slewing correction is based on the difference between the high- and low-threshold crossing times; if only the low threshold is crossed, the slewing correction is based on a fit to the measured distribution of leading-edge time vs. time-over-threshold. After the application of slewing corrections, time resolutions at the level of 1 ns or better are obtained for all LAV stations, as shown in Fig. LAV-4. We note that these results are obtained with samples including all hit edge configurations: not only complete hits built from leading/trailing edge pairs for both thresholds, but also hits crossing only the low threshold.

We have attempted to study the detection efficiency for photons using a clean sample of $K^+ \rightarrow \pi^+ \pi^0$ decays in which the π^+ track is reconstructed, one of the two photons from the π^0 is detected as an LKr calorimeter cluster, and the second photon is expected to be found in one of the LAV detectors on the basis of kinematic closure. At present, the resolution on the extrapolated direction of the photon is not sufficient to allow the efficiency to be determined for individual LAV stations; this may be possible in the future by means of a complete kinematic fit making use of all available information on the K^+ trajectory from the Gigatracker. As a first attempt, we have focused on estimating the global efficiency for the entire LAV system. We thus consider events to be successfully matched if they contain at least one LAV block fired within 5 ns of the $K^+ \rightarrow \pi^+ \pi^0$ event time from the reference detector. MC studies demonstrate that the photon detection inefficiency as determined by this method is dominated by geometrical inefficiencies and upstream photon conversions;

the intrinsic inefficiency arising from the LAV detectors itself is less than one-sixth of the observed inefficiency. Relying on the MC estimate for the contribution from the former effects, we find the intrinsic inefficiency to be a few 10^{-3} , with about 5% of the detected photons observed as a signal on an isolated block crossing only the low threshold. These results are preliminary; as noted above, further refinements to the method will be implemented. We note, however, that obtaining an accurate tag for the determination of the single-photon detection efficiency at the level of 10^{-3} or lower is difficult; determination of the experiment's π^0 overall rejection power is both easier and more relevant for the measurement of BR $K^+ \rightarrow \pi^+ \nu \bar{\nu}$

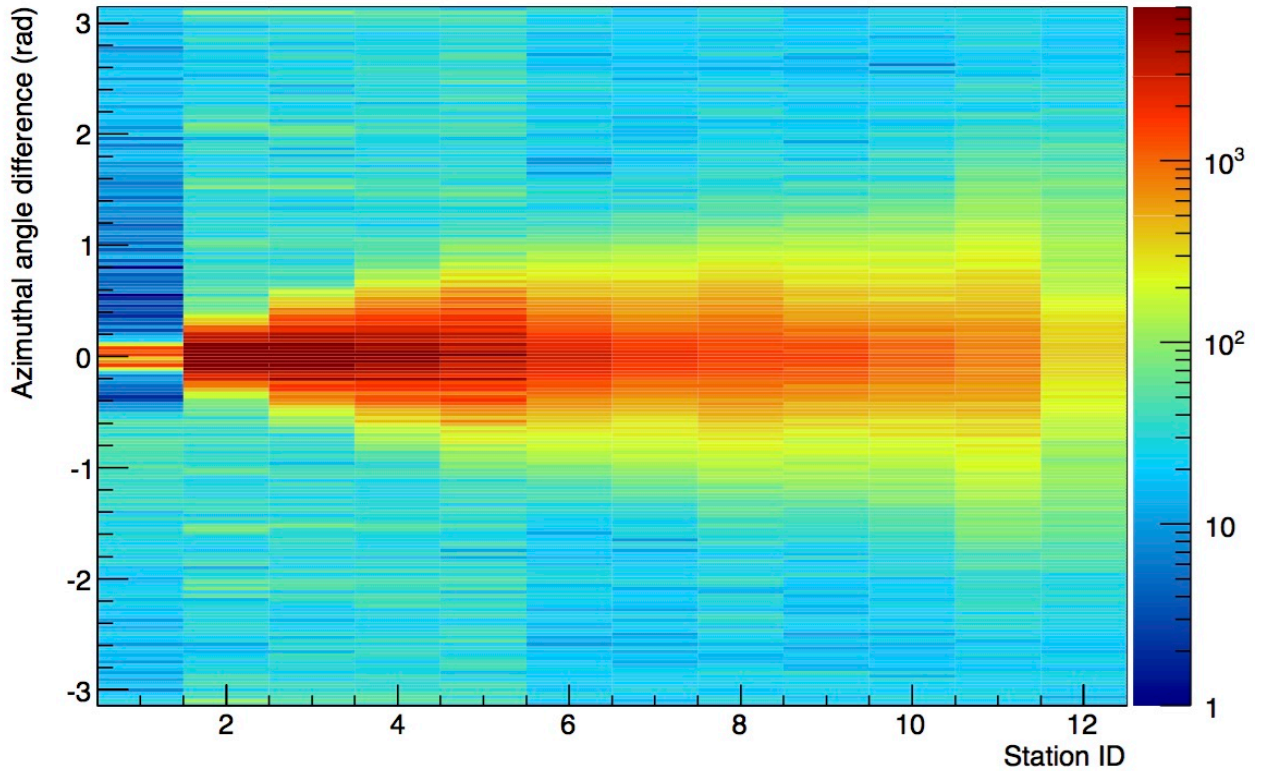


Figure LAV-2. Distribution of difference in azimuth, $\Delta\phi$, between clusters on different stations vs. the number of stations between the most upstream and downstream clusters.

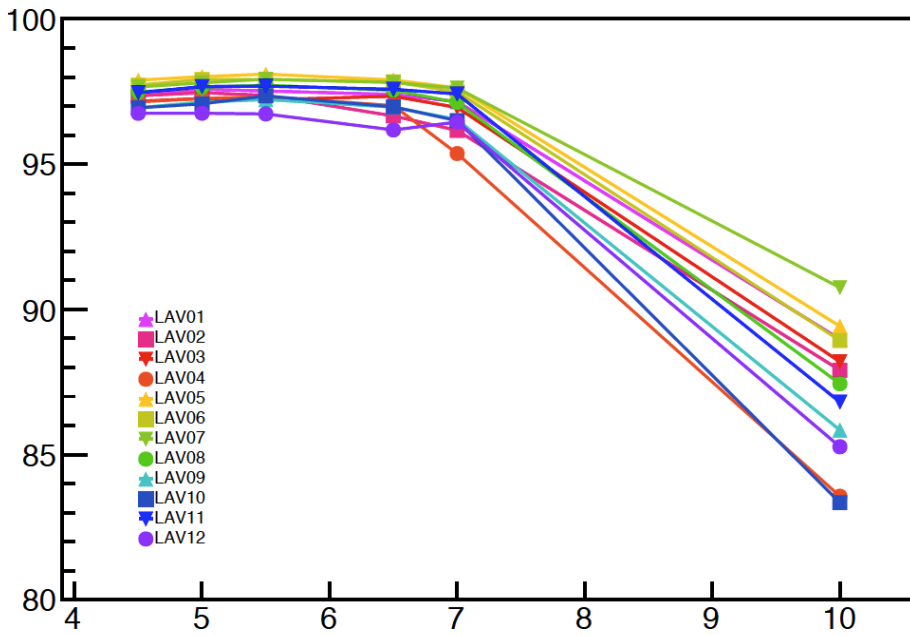


Figure LAV-3. Average MIP detection efficiency for different stations as a function of threshold.

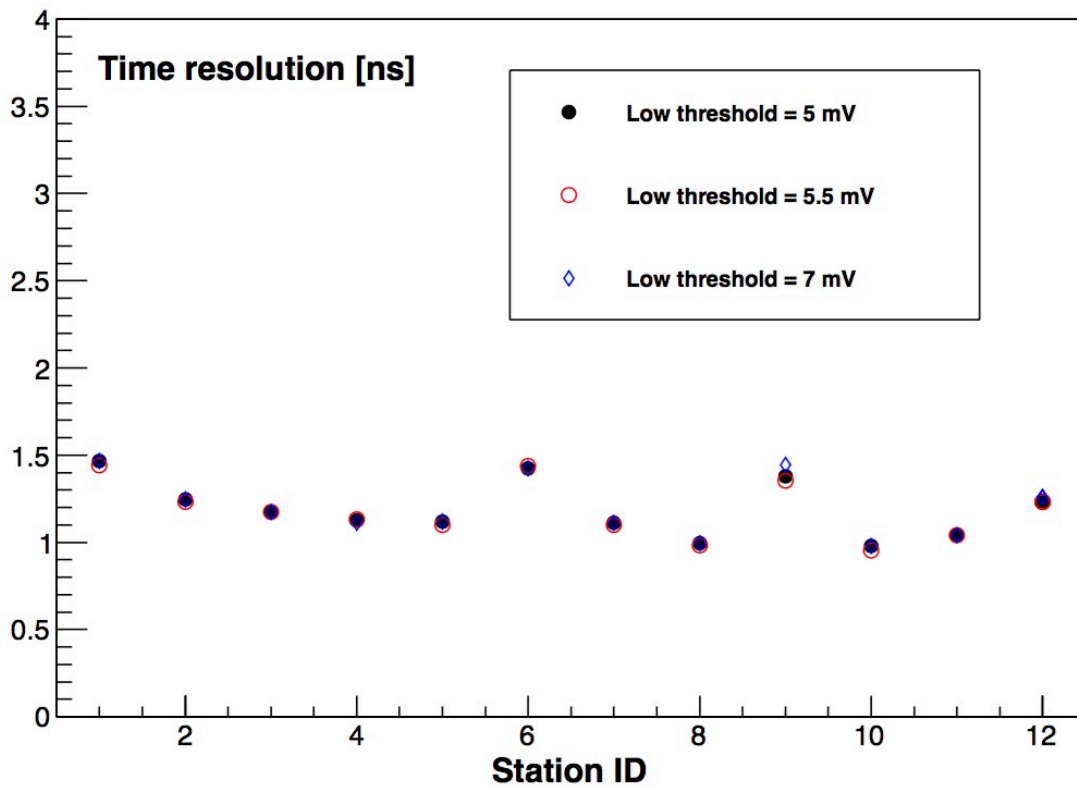


Figure LAV-4. Difference between LAV hit time and event time from KTAG (ns) for different thresholds, for the twelve stations.

LNF group activity: SAC and IRC

The small-angle veto detectors, SAC and IRC, are shashlyk type electromagnetic calorimeters that provide veto coverage for photons with polar angles down to zero degrees. They are exposed to a very high rate of photons from kaon decays and, for the IRC, muons from pion and kaon decays. After a comprehensive design review in early 2014, the IRC was assembled at Frascati and shipped to CERN for installation before the first NA62 run.

During this year the following tasks were accomplished:

- Commissioning of the IRC
- Analysis of 2015 data and evaluation of the SAC and IRC performance.

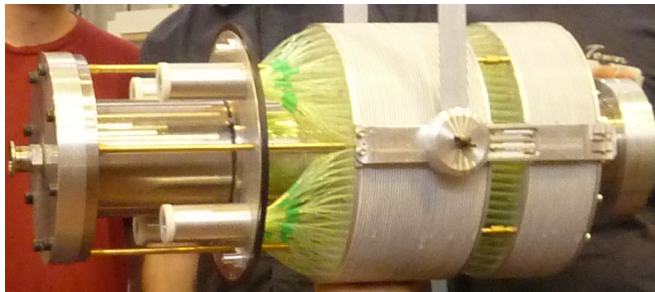


Figure SAV-1. The IRC assembly before shipping to CERN.

Both the SAC and the IRC were installed August and September 2014. They were aligned to a precision of better than 1 mm for each of the reference rod holes, since the IRC is the closest downstream detector to the beam axis, and the 23-mrad rotation angle of the SAC is necessary for high efficiency, to eliminate the possibility of photons escaping longitudinally via the through holes for the fibers.

Both detectors were operated from the beginning of the run. The signals were read out with the standard NA62 readout system, based on the LAV-FEE and TEL62 boards, as described above. As for LAV12, L0 primitives were generated for the IRC and SAC. Copies of the IRC and SAC signals were also provided to the LKr calorimeter readout modules, so that the SAC and IRC were also available for use in the L0 trigger from the calorimeter readout chain.

A simple online monitor was implemented for the SAC and IRC, based only on the total normalized rate, defined as the total number of hits in each detector normalized to the total number of recorded events for each burst, as shown in Figure SAV-2. This allowed monitoring of changes in the trigger definition and beam alignment, in addition to the proper operational status of the detectors.

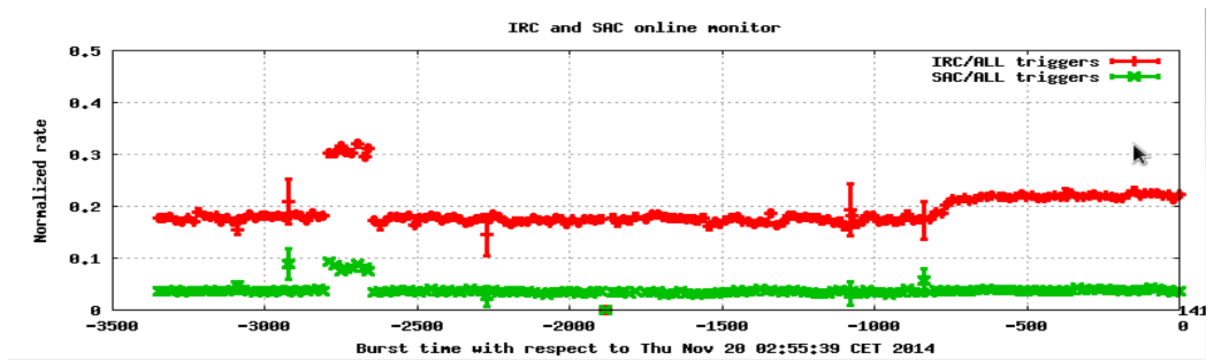


Figure SAV-2. The online monitor for the SAC and IRC.

The response of both detectors to MIPs was studied with data from the muon runs discussed in the previous section. The SAC and IRC event rates for different thresholds were fit with a cumulative Landau distribution function. The most probable value for the MIP signal amplitude was found to be around 4 mV, which is consistent with expectation, and stable in both data sets. The time resolution for muons was better than 2 ns for the SAC and better than 1.6 ns for the IRC, while the time resolution measured with tagged photons from $K^+ \rightarrow \pi^+ \pi^0$ decays was better than 1 ns.

1) Study of the $K^+ \rightarrow \pi^+ \gamma \gamma$ decay by the NA62 experiment
C.Lazzeroni, et al, NA62 Collaboration, **Physics Letters B 732C (2014)**

CONFERENCE TALKS

PhiPsi2015, Hefei, Anhui, China, 23-26 Sep 2015, Francesco Gonnella: Search for the dark photon in π^0 decays

13th Pisa meeting on advanced detectors, Isola d'Elba, Italy, 24-30 May 2015, Gianluca Lamanna: Graphics Processing Units for HEP trigger systems (including tests performed at NA62)

CIPANP 2015, Vail, Colorado, USA, 19-24 May 2015, Silvia Martellotti: The NA62 experiment at CERN

29th Rencontres De Physique De La Vallée D'Aoste, La Thuile, Aosta, Italy, 1-7 Mar 2015, Mauro Raggi: First observation of $K^+ \rightarrow \pi^+ \pi^0 e^+ e^-$

Lake Louise Winter Institute 2015, Lake Louise, Alberta, Canada, 15-21 Feb 2015, Francesco Gonnella: Status of the NA62 experiment